Characterization of stony soils' hydraulic conductivity using laboratory and numerical experiments

E. Beckers[1], M. Pichault[1, 2], W. Pansak[3], A. Degré[1], S. Garré[2]

[1] Université de Liège, Gembloux Agro-Bio Tech, UR Biosystems Engineering, Passage des déportés 2, 5030 Gembloux, Belgium

[2] Université de Liège, Gembloux Agro-Bio Tech, UR TERRA, Passage des déportés 2, 5030 Gembloux, Belgium

[3] Naresuan University, Department of Agricultural Science, 65000 Phitsanulok, Thailand

Correspondence to: S. Garré (sarah.garre@ulg.ac.be)

Abstract

Determining soil hydraulic properties is of major concern in various fields of study. Although stony soils are widespread across the globe, most studies deal with gravel-free soils so that the literature describing the impact of stones on the hydraulic conductivity of a soil is still rather scarce. Most frequently, models characterizing the saturated hydraulic conductivity of stony soils assume that the only effect of rock fragments is to reduce the volume available for water flow and therefore they predict a decrease in hydraulic conductivity with an increasing stoniness. The objective of this study is to assess the effect of rock fragments on the saturated and unsaturated hydraulic conductivity. This was done by means of laboratory experiments and numerical simulations involving different amounts and types of coarse fragments. We compared our results with values predicted by the aforementioned predictive models. Our study suggests that considering that stones only reduce the volume available for water flow might be ill-founded. We pointed out several drivers of the saturated hydraulic conductivity of stony soils, not considered by these models. On the one hand, the shape and the size of inclusions may substantially affect the hydraulic conductivity. On the other hand, laboratory experiments show that an increasing stone content can counteract and even overcome the effect of a reduced volume in some cases: we observed an increase in saturated hydraulic conductivity with volume of inclusions. These differences are mainly important near to saturation. However, comparison of results from predictive models and our experiments in unsaturated conditions shows that models and data agree on a decrease in hydraulic conductivity with stone content,

even though the experimental conditions did not allow testing for stone contents higher than 20%.

Keywords: stony soils, hydraulic conductivity, evaporation method, hydrodynamic behaviour, permeameter, soil water content.

1. Introduction

Determining soil hydraulic properties is of primary importance in various fields of study such as soil physics, hydrology, ecology and agronomy. Information on hydraulic properties is essential to model infiltration and runoff, to quantify groundwater recharge, to simulate the movement of water and pollutants in the vadose zone, etc. (Bouwer and Rice, 1984). Most unsaturated flow studies characterize the hydraulic properties of the fine fraction (particles smaller than 2 mm of diameter) of supposedly uniform soils only (Bouwer and Rice, 1984; Buchter et al., 1994; Gusev and Novák, 2007). Nevertheless, in reality, soils are heterogeneous media and may contain coarse inclusions (stones) of various sizes and shapes.

Stony soils are widespread across the globe (Ma and Shao, 2008) and represent a significant part of the agricultural land (Miller and Guthrie, 1984). Furthermore, their usage tends to increase because of erosion and cultivation of marginal lands (García-Ruiz, 2010). Yet little attention has been paid to the effects of the coarser fraction on soil hydraulic characteristics, so that the relevant literature is still rather scarce (Ma and Shao, 2008; Novák and Šurda, 2010; Poesen and Lavee, 1994).

Many authors consider that the reduction of volume available for water flow is the only effect of stones on hydraulic conductivity. This hypothesis has led to models linking the hydraulic conductivity of the fine earth to those of the stony soils. They predict a decrease in saturated hydraulic conductivity of stony soil (K_{se}) with an increasing volumetric stoniness (R_v) (Bouwer and Rice, 1984; Brakensiek et al., 1986; Corring and Churchill, 1961; Hlaváčiková and Novák, 2014; Novák and Kňava, 2011; Peck and Watson, 1979; Ravina and Magier, 1984).

However, a number of studies do not observe this simple relationship between the hydraulic conductivity and the stoniness (Zhou et al., 2009; Ma et al., 2010; Russo, 1983; Sauer and Logsdon, 2002) and suggest that other factors may play a substantial role in specific situations. Indeed, ambivalent phenomena can intervene simultaneously, which makes the understanding of the effective hydraulic properties of stony soils difficult. The reduced volume available for flow might be partially compensated by others factors. One contradictory effect might be, as pointed out by Ravina and Magier (1984), the creation of large pores in the rock fragments' vicinity. Indeed, the creation of new voids at the stone-fine earth interface could generate preferential flows and hence increase the saturated hydraulic conductivity (Zhou et al., 2009; Cousin et al., 2003; Ravina and Magier, 1984; Sauer and Logsdon, 2002).

These statements define the general context in which our study takes place. The main objectives are (i) to assess the effect of rock fragments on the hydraulic conductivity of soil and (ii) to test the validity of the aforementioned models.

2. Material and Methods

We studied the effect of R_v on saturated and unsaturated hydraulic conductivity by means of laboratory experiments (evaporation and permeability measurements) and numerical simulations involving different amounts and types of coarse fragments. The latter serve also to further investigate the effect of the stone size and shape on the K_{se}.

2.1. Models predicting soil hydraulic properties of stony soils

Multiple equations have been proposed to estimate the saturated hydraulic conductivity of stony soil (K_{se}) from the one of the fine earth (K_s) assuming that rock fragments only decrease the volume available for water flow. The relative saturated hydraulic conductivity (K_r) is defined as the ratio between the K_{se} and the K_s. Eq. (1) and Eq. (2) have been derived by Peck and Watson (1979) based on heat transfer theory for a homogeneous medium containing non-porous spherical and cylindrical inclusions, respectively. Assuming that stones are non-porous and do not alter the porosity of the fine earth, Ravina and Magier (1984) approximated the K_r to the volumetric percentage of fine earth (Eq. (3)). Based on empirical relations, Brakensiek et al. (1986) proposed a similar equation, but involving the mass fraction of the rock fragments instead of the volumetric fraction (Eq. (4)). On the basis of numerical simulations, Novák et al. (2011) proposed to describe the K_{se} of stony soils as a linear function of the R_v and a parameter that incorporates the hydraulic resistance of the stony fraction (Eq. (5)).

$K_r = \frac{2(1-R_v)}{2+R_v}$	$K_r = \frac{(1-R_v)}{1+R_v}$	$K_r = (1-R_v)$	$K_r = (1-R_w)$	$K_r = (1-aR_v)$
(1)	**(2)**	**(3)**	**(4)**	**(5)**
Peck and Watson for spherical stones (1979)	Peck and Watson for cylindrical stones (1979)	Ravina and Magier (1984)	Brakensiek et al. (1986)	Novák et al. (2011)

In which R_v is the volumetric stoniness [$L^3.L^{-3}$]; R_w is the mass fraction of the rock fragment (mass of stones divided by the total mass of the soil containing stones; the stone density is typically 2.5 g/cm^3 in this case) [$M.M^{-1}$]; a is an empirical parameter that incorporates the hydraulic resistance of the stony fraction considering shape, size and orientation of inclusions (the recommended value is 1.32 for clay soils according to Novák et al. (2011)).

Two major characteristics are widely used to describe the hydraulic properties of unsaturated soil: the water retention curve $\theta(h)$ and the hydraulic conductivity curve $K(h)$. These are both non-linear functions of the pressure head h. One of the most commonly used analytical models has been introduced by van Genuchten (1980), based on the pore-bundle model of Mualem (1976), and given by:

$$S_e(h) = \frac{\theta(h) - \theta_r}{\theta_s - \theta_r} = \begin{cases} (1 + |\alpha h|^n)^{-m} \; if \; h < 0 \\ 1 \; if \; h \geq 0 \end{cases} \quad (6)$$

$$K(S_e) = \begin{cases} K_s \, {S_e}^l \left[1 - (1 - {S_e}^{1/m})^m\right]^2 \; if \; h < 0 \\ K(S_e) = K_s \; if \; h \geq 0 \end{cases} \quad (7)$$

In which h is the pressure head [L]; $S_e(h)$ is the saturation state [$L^3.L^{-3}$]; $\theta(h)$ is the volumetric water content [$L^3.L^{-3}$]; θ_r and θ_s respectively represent the residual and saturated water content [$L^3.L^{-3}$]; K_s is the saturated hydraulic conductivity [$L.T^{-1}$]; n [-], l [-], α [L^{-1}] are empirical shape parameters ($m = 1 - 1/n, n > 1$). To extend the hydraulic conductivity curves to stony soils, Hlaváčiková and Novák (2014) propose a simple method considering that the shape parameters of the van Genuchten/Mualem (VGM) equations (α, n and l) are independent of R_v. However, this model relies on assumptions that have not been verified. It might be noteworthy to mention that there are currently no extensive empirical studies available dealing with the influence of porous inclusions under unsaturated conditions. This gap in existing literature is probably due to experimental issues linked with this kind of study: while measuring the potential and the water content of fine earth has become a standard procedure, the opposite is true for rock fragments, especially under transient infiltration processes.

2.2. Laboratory Experiments

2.2.1. Sample Preparation

We performed laboratory experiments on disturbed samples (height: 65 mm, diameter: 142 mm) containing a mixture of fine earth and coarse inclusions. Two types of inclusions were used: rock fragments (granite) with a diameter between 1 and 2 cm (1) and spherical glass beads with a diameter of 1 cm (2) (see fig 1). The fine earth is classified as a clay (sand: 26%, silt: 19%, clay: 55%).

Before each measurement campaign, fine earth was first oven dried for 24 hours at 105°C and passed through a 2-mm sieve. To prepare a sample without any inclusion, fine earth was compacted layer-by-layer to get an overall bulk density of 1.51 g/cm^3 (equal to the mean bulk density of the fine earth measured in situ (Pichault, 2015)). For samples containing rock

fragments, stones were divided over four layers of soil application and laid on the fine earth bed on their flattest side. The samples were then compacted layer-by-layer in a way that maintains the same bulk density of fine earth as for samples without inclusions. Even though the filling and compaction procedure was conducted with precision, it is probably impossible to avoid local bulk density heterogeneity as stones can move and/or soil between stones can be less compacted due to difficult access of the area close to the stone during compaction. The same procedure was to prepare samples containing glass balls. Once the specimen was made, it was placed in a basket containing a thin layer of water during at least 24 hours in order to saturate the soil from below.

2.2.2. Unsaturated Hydraulic Conductivity

Setup Description

We used the evaporation method to determine the hydraulic conductivity and the retention curve of a soil sample. The principle of this method is to simultaneously measure the matric head at different depths and the water content of an initially saturated soil sample submitted to evaporation.

The experiments were performed using cylindrical Plexiglas samples of 1 L (height: 65 mm, diameter: 142 mm), perforated at the bottom to allow saturation from below and open to atmosphere on the upper side to allow evaporation of the soil moisture. Four 24.9 mm-long and 6mm diameter ceramic tensiometers (SDEC230) were introduced at 10, 25, 40 and 55 mm in height, respectively denoted T1 to T4 (the reference level is located at the bottom of the sample). Tensiometers are introduced at saturation; a pin with similar dimensions is used to facilitate their insertion. In order to avoid preferential flow due to the introduction of the tensiometers on the same vertical axis, each tensiometer was introduced with a horizontal shift of 12 degrees with respect to the center of the column. The tensiometers are connected by a tube to a pressure transducer (DPT-100, DELTRAN). The setup was filled with degassed water. The variation in pressure of the drying soil was recorded every 15 min by a CR800 logger (CAMPBELL SCIENTIFIC). Tensions beyond the air entry point were not taken into account. The air entry point refers to the state from which the measured pressure head starts to decrease as bubbles appear and water vapour accumulates (typically 68 kPa in this case).

The total water loss as a function of time was monitored by a balance (OHAUS) with a sensitivity of 0.2 g with an accuracy of $\pm$ 1 g with a time resolution of 15 min. A 50 W infrared lamp was positioned 1 m above the sample surface to slightly speed up the evaporation process.

The light was turned off for the first 24 hours of every experiment, as the evaporation rate is already high in a saturated sample. A measuring campaign lasted until three of the four tensiometers ran dry (the tension sharply drops down to approximately a null value). At the end of the experiment, the sample was oven dried for 24 hours at 105°C to estimate the θ.

Data Processing

A simplified Wind's method (1968) was used to transform matric potential and total weight data over time into the hydraulic conductivity curve (Schindler, 1980 cited by Schindler and Müller, 2006; Schindler et al., 2010). The method is further adapted in order to take into account the data from four tensiometers. The method assumes that the distribution of water tension and water content is linear through the soil column. It further linearizes the water tension and the mass changes over time. The time step chosen to process the data is one hour.

By calculating the hydraulic conductivity based on measurements of two tensiometers and linking it to the corresponding mean matric head, one can evaluate a point of the hydraulic conductivity curve. We used every possible combination of two tensiometers (six here) to obtain data points for the hydraulic conductivity curve.

Points of the hydraulic conductivity curve obtained at very small hydraulic gradients (defined here as $\nabla K = \frac{\Delta|h|}{\Delta z} - 1$) were rejected, because large errors occur in the near-saturation zone due to uncertainties in estimating small hydraulic gradients (Peters and Durner, 2008; Wendroth, 1993). This highlights in its turn the necessity of reliable tensiometers to estimate the near-saturated hydraulic conductivity. In the current literature, acceptation limits of the hydraulic gradient vary between 5 and 0.2 cm/cm (Mohrath et al., 1997; Peters and Durner, 2008; Wendroth, 1993). Using the least restrictive filter criterion (hydraulic gradient > 0.2) requires fine calibration and outstanding performance of the tensiometers. Choosing a more restrictive criterion leads to a larger loss of conductivity points, but provides more reliable and robust data. We decided to use a filter criterion that does not consider hydraulic conductivity points higher than the evaporation rate (from 0.1 to 0.2 cm/day in this case), resulting in a lower limit of 1 cm/cm for the hydraulic gradient.

As pointed out by Wendroth (1993) and Peters and Durner (2008), the main drawback associated with the evaporation experiment is that no estimates of conductivity in the wet range can be obtained due to the typically small hydraulic gradients so that additional measurements of the K_{se} should be provided. To do so, we used constant-head permeability experiments (see below). Except for the K_{se} which is fixed using results from the constant-head permeability

experiments, the parameters of the VGM-model (1980) (Eq. (7)) are obtained by fitting evaluation points from each combination of tensiometers using the so-called "integral method" (Peters and Durner, 2006).

2.2.3. Saturated Hydraulic Conductivity

Constant-head permeability experiments were used to determine the K_{se} of saturated cylindrical core samples. The flow through the sample is measured at a steady rate under a constant pressure difference. The K_{se} can thus be derived using the following equation:

$$K_{se} = \frac{VL}{A\Delta H\Delta t} \tag{12}$$

In which V is the volume of discharge [L^3]; L is the length of the permeameter tube [L]; A is the cross-sectional area of the permeameter [L^2]; ΔH is the hydraulic head difference across the length L [L] and Δt is the time for discharge [T].

The soil sample used for permeability tests has the same size as the one from the evaporation experiment (height: 65mm, diameter: 142 mm). A 2 cm thick layer of water was maintained on top of the sample thanks to a Mariotte bottle. Water was collected through a funnel in a burette and the volume of discharge V was deduced from measurements after 30 and 210 min after the beginning of the experiment (Δt= 180 min).

2.3. Numerical simulations

The HYDRUS-2D software was used to simulate water flow in variably saturated porous stony soils. HYDRUS-2D is a two-dimensional finite element model based on Richard's equation.

All the performed simulations assumed that rock fragments were non-porous so that "no-flux" boundaries conditions were specified along the stones limits. Rock fragments were supposed to be circular. The soil domain over which simulations were performed had the same dimensions as the longitudinal section of the sampling ring used in the laboratory experiments (14 x 6.5 cm). We considered the 2D fraction of stoniness equal to the volumetric fraction. The parameters of fine earth used in the simulations come from the fitting on the hydraulic conductivity and water retention curves obtained in our laboratory experiments on stone-free samples (Table 1).

As a general rule, the hydraulic conductivity of a heterogeneous medium tends to be higher for 3D than for 2D simulations (Dagan, 1993). Similarly, for a same level of heterogeneity, the

flow will be more hampered using 1D rather than 2D simulations. In the present study, we performed 2D simulations: the quantitative and qualitative conclusions from these experiments can be only extended to the third dimension for their corresponding 3D form with an infinitely long axis.

2.3.1. Unsaturated Hydraulic Conductivity

We repeated the evaporation experiment as numerical simulation. The top boundary of the simulated sample was submitted to an evaporation rate q of 0.1 cm/day during 14 days. No fluxes were allowed across other boundaries. The calculation method applied to the output data was similar to the laboratory evaporation experiment, except that the conductivity and pressure head estimations resulted from two observation nodes placed at the top and the bottom of the profile. We are aware that these choices can be discussed, because of numerical instability at the limits of the sample on the one hand, and because of the setup extension modelled here (see Peters et al., 2015) on the other hand. However, we chose to consider these points for different reasons. Indeed, we observed some numerical instability near stones, which makes it more complicated to insert nodes deeper in the sample, especially for increasing stone contents. Besides, we checked that pressure head was linearly distributed across the soil profile, which was the case. Finally, as we are studying clayey soils, and as we are considering a pressure head range between pF 1.5 ad 2.5 these assumptions are likely to be fair enough (Peters et al., 2015).

As the relative mass balance error was large at the beginning of the simulations, we considered values when this relative error was lower than 5%. This validation criterion was set arbitrarily, based on the comparison between evaluation points from the simulation of the evaporation experiment on stone-free samples and the expected values obtained from the inputs of the simulation. The hydraulic conductivity curve was obtained fitting the discrete conductivity data plus the simulated saturated hydraulic conductivity using the so-called “integral method” (Peters and Durner, 2006), just like we did for the laboratory experiment.

2.3.2. Saturated Hydraulic Conductivity

The K_{se} was determined using a numerical constant-head permeability simulation. We simulated a steady-state water flow of a saturated soil profile, with a constant head of 10 cm applied on the upper boundary. The bottom boundary of the column was defined as a “seepage face”, which means that water starts flowing out as soon as the soil at the boundary reaches

saturation. The calculation method applied to the output data was identical to the permeability experiment.

2.4. Treatments

Table 2 presents a scheme of all the performed experiments. We first studied the effect of R_v on unsaturated hydraulic properties using laboratory experiments and numerical simulations. In the laboratory approach, we performed evaporation experiments on samples containing i) fine earth only and ii) on others with rock fragments (1) at a R_v of 20%. Two replications per treatment were performed (four measurement campaigns in total). For the numerical approach, simulations of the evaporation experiment were done on homogeneous soil (without stones) and on soil with a R_v of 10, 20 and 30%. Having less time- and practical constraints in the numerical simulation, we added an increasing R_v to observe the evolution of the hydraulic conductivity curve. Simulations were performed on soil samples containing 12 regularly distributed stones. One can notice that no investigations of the unsaturated properties with coarse fragments above 30% of R_v were performed. Indeed, given that small variations of the hydraulic gradient can lead to substantial changes in the hydraulic conductivity estimates, the tensiometers should be ideally positioned out of the direct influence of one particular stone in order to obtain generalizable results. This implies the need for relatively low stone contents (< 30% according to Zimmerman and Bodvarsson (1995)).

Then, to study the relationship between K_{se} and R_v, we tested two types of inclusions (rock fragments (1) and glass spheres (2)) and four volumetric fractions (0, 20, 40 and 60%). We did not perform any replications for glass sphere inclusions while five replications were performed for rock fragments. The first setup with rock fragments was concomitant with the one with glass spheres. Then, the four supplementary replications with rock fragments were processed for the different volumetric fractions altogether: between replications the soil was oven dried for 24 hours at 105°C and passed through a 2-mm sieve. Numerical permeability simulations were also performed involving 12 circular regularly distributed inclusions for the same R_v (0, 20, 40, 60%).

In addition, we used simulations to investigate the effect of the inclusion shape and size on K_{se}. To do so, simulations of the permeability test were performed on soil containing stones of five different shapes: circular, upward equilateral triangle, downward equilateral triangle, rectangle on its shortest side (L x 1.5L) and rectangle on its longest side (1.5L x L)) with an R_v of 10, 20 and 30%. We first performed simulations on soil containing only one centered inclusion. We

also performed permeability simulations on soil containing 12 and 27 regularly distributed inclusions (for each R_v).

3. Results and Discussion

In the following, results from laboratory experiments and numerical simulations will be compared to the predictions of the different models developed in Section 2.1. The K_{se} will be represented by the median value predicted by the five models linking the properties of fine earth to the ones of stony soil (Eq. (1) to Eq. (5)). This will be referred to as "results from the K_{se} predictive models" in the following and will be graphically represented by dotted lines. The same predictive models assume that the shape parameters of the VGM-equations, *n*, *l* and α, do not depend of the stoniness, as suggested by Hlaváčiková and Novák (2014). As mentioned above, unsaturated functions of stony soils have been barely studied. We will compare results from unsaturated experiments and numerical simulations to predictive models results following this assumption.

3.1. Effect of Stones on Saturated Hydraulic Conductivity

Fig. 2 shows the relationship between the saturated hydraulic conductivity (K_{se}) and the volumetric stone content (R_v) obtained from the constant-head permeability tests for laboratory experiments and numerical simulation (12 circular inclusions). The figure also depicts the median K_{se} of the predictive models (dashed line) and the bars show the 95% intervals around the median predicted by these models.

The models predict a decreasing K_{se} for an increasing R_v. The numerical simulations show a decrease in K_{se} with an increasing R_v, similar to the predictive models. Looking at the average curve obtained with our five replications (fig 2), we observe an overall increase between a R_v of 0 and 60%, this global trend being observed for each replication individually (fig 3). Statistically speaking, there are significant differences between K_{se} at a R_v of 0 and 60% and between K_{se} at a R_v of 20 and 60%. However, at low stone content, we observe for some replications local decrease of K_{se}. For example, for the first replication (Gravels 1, fig 3) K_{se} decreases until a R_v of 20% and then K_{se} begins to increase. For the second replication (Gravels 2, fig 3), the K_{se} increases from a R_v of 0 to 20% and then decreases at a R_v of 40%. Analogous permeability tests conducted by Zhou et al. (2009) showed a similar behaviour: the K_{se} initially decreases at low rock content to a minimum value at R_v = 22% and then at higher R_v, K_{se} tends to increase with R_v. Other laboratory tests carried out by Ma et al. (2010)

displayed a larger K_{se} at R_v = 8% than the one of the fine earth alone. While carrying out in situ infiltration tests, Sauer and Logsdon (2002) measured higher K_{se} with increasing R_v, but decreasing K with increasing R_v under unsaturated conditions (and particularly at h = -12 cm). These considerations suggest that the relationship between K_{se} and R_v proposed by the predictive models simplifies reality to a great extent. These contradictory results suggest that the variation of K_{se} depends on different factors that can counteract the reduction of the volume available for water flow. One possible explanation of our observations has been pointed out by Ravina and Magier (1984), who directly observed large voids by cutting across a stony clay soil sample after its compaction, presumably due to translational displacement of densely packed fragments. This compaction of a saturated sample creates voids near the stone surface and hence increases K_{se} with an increasing R_v. Our sampling procedure, demanding the compaction of the sample layer-by-layer, could lead to the same kind of phenomena observed by Ravina and Magier (1984). Besides, we have to keep in mind that these elements are very likely to have a different impact depending on soil texture, which was clay for both studies.

Glass beads were used to check the influence of rock characteristics on our conclusions about K_{se}. Since results with glass beads show a trend similar to the five replications with rock fragments, we infer that it is not the rock fragment itself that produces bigger K_{se}, but the presence of a certain volume of inclusions. Besides, the variation observed between the trends of the curves with rock fragments and glass beads could be due to the inner variation of the hydraulic properties of samples, but it could suggest as well that K_{se} depends on the shape and the roughness of the inclusions. Nevertheless, we can only see the combined effect of these factors in this experiment. This leaves the understanding of the major drivers of the K_{se} and their relative importance unclear. These elements are further investigated through numerical simulations.

Besides the observed increase of K_{se} depending on rock content, we can also observe a decrease in K_{se} between replications (see fig 3). In fact, as mentioned above, the global trend of increasing K_{se} is observed for each replication individually, but sampling procedure seems to have a large impact on results too. There are significant differences ($p<0.05$) between replication 2 and replication 5, the last one presenting lower K_{se}. The drying and wetting cycles and/or the sieving influence the hydrodynamic behavior of soil fraction since the effect decreases when R_v increases. This underlines the effect of soil texture and is an important aspect to take into account in future studies.

3.2. Effect of the Stone Size and Shape on the Saturated Hydraulic Conductivity

To investigate the effect of the size of the inclusions and their shape on K_{se} separately from other factors of variation, we performed constant-head permeabiltiy simulations on samples containing 1, 12 and 27 inclusions of various shapes, for a R_v of 10, 20 and 30%. Table 3 illustrates the tendency of the effects and their respective drivers.

Table 3 presents the K_r for different sizes of circular inclusions and increasing overall stone content (R_v). When the size of the inclusions decreases (when the number of inclusions increases for a same R_v), the K_r tends to decrease. An interaction between the R_v and the size of inclusion can be observed: the effect of size is more marked with a higher R_v. For example, the decrease in K_r between 1 and 27 circular inclusions is limited to 2% for a R_v of 10%, but rises up to 25% for a R_v of 30%. A similar behavior is observed with simulations for different shapes of inclusions. These statements support the findings of Novák et al. (2011): the smaller the stones, the higher the resistance to flow at a given stoniness. We suggest the decrease of K_{se} is due to a combination of the two following phenomena. The first one is the overlapping of the influence zone of each inclusion, causing further reduction of K_r. The concept of overlapping influence zones was first proposed by Peck and Watson (1979) to explain higher decrease of the hydraulic conductivity of stones very close to each other in comparison to isotropically distributed stones. The second phenomenon could be that, for a given R_v, the contact area between stones and fine earth is higher for small stones than for bigger ones. Hence, a higher tortuosity can be responsible for a lower flow rate.

The shape of the inclusions also has a visible impact on K_r. For a fixed number of inclusions, the K_r is higher with rectangular inclusions on their shortest side and smaller with rectangular inclusions on their longest side. Circular inclusions provoke a smaller reduction than triangular inclusions. The orientation of the triangles does not have a pronounced effect on K_r. Here again, we observe a stronger effect of the size for higher stoniness. As an illustration, the decrease in K_r between circular and triangular inclusions is limited to 5% for a R_v of 10% but rises up to 14% for a R_v of 30%. A similar behavior is observed with simulations including either 1 or 27 fragments.

Considering a fixed R_v of 20% (see Table 3), the effect of the shape of the inclusions depends on their size. For example, the decrease in K_r between rectangular inclusions positioned on their longest and shortest sides is limited to 13% for samples containing one inclusion only while it is as high as 21% for samples containing 27 inclusions. Inversely, the effect of the size

of inclusions also depends on their shape. This effect is higher for triangular and rectangular inclusions positioned on their longest side, with a K_r decrease between 1 and 27 inclusions of 23 and 18% respectively. This effect is less significant for circular inclusions, and for rectangular inclusions positioned on their shortest sides. The associated K_r decrease between 1 and 27 inclusions is 11 and 10% respectively.

The median value of K_r predicted by the models for a R_v of 20% (0.73) is similar to the simulated K_r for samples containing only one spherical inclusion (Table 3). The K_r predicted by the models is always higher than the K_r determined by the simulations, except for soils containing one inclusion on its shortest side. This can be a side effect of 2D simulations versus 3D measurements. Nevertheless, the numerical simulations show that the shape and the size of inclusions may have an effect on K_{se}, which is usually neglected by the current predictive models. In general there is a concordance between models and simulations, whatever shape and orientation of stones. This strengthens our hypothesis that macropore creation or heterogeneity of bulk density close to the stones can occur and influence K_{se}. Indeed, numerical simulations cannot simulate the creation of voids, unless we create them manually and subjectively in the domain.

Eventually, we hypothesize that, from a certain R_v onwards – the exact R_v value depending on the sampling procedure, the shape and roughness of inclusions, as well as soil texture – stoniness is at the origin of a modification of pore size distributions and of a more continuous macropore system at the stone interface. This macropore system could overcome the other drivers reducing K_{se} .

3.3. Effect of Stones on Unsaturated Hydraulic Conductivity

Fig. 4 represents the hydraulic conductivity curves obtained from the permeability and evaporation simulations for different stoniness (R_v = 0, 10, 20 and 30%) as well as results predicted by the models for the corresponding R_v. The hydraulic conductivity curves from the predictive models and from the numerical simulations match hydraulic conductivity decreases for increasing R_v. According to these simulations, hydraulic conductivity in the unsaturated zone is well defined using a correct K_{se} and shape parameters do not depend on the stoniness. But this is not surprising since predictive models and numerical simulations rely on same assumptions, i.e imperviousness of stones and an identical porosity distribution of fine earth. As a result, these elements do not prove that shape parameters do not depend on the stoniness.

Fig. 5 represents the hydraulic conductivity curves obtained from laboratory experiments on stone-free samples and on samples with a R_v of 20% as well as the results predicted by the models for a R_v of 20%. Even though the data points are dispersed, those coming from the evaporation experiments measured on stony samples are globally lower and slightly more flattened than the ones measured on stone-free samples. This suggests that stones decrease unsaturated hydraulic conductivity. However, it must be noted that we do not have unsaturated K data for higher stone contents, whereas for K_{se}, the effect becomes more obvious for R_v > 20%. It might therefore be needed to find a way to conduct evaporation experiments for higher stone contents in order to draw final conclusions.

In the numerical simulations, the presence of stones reduces the hydraulic conductivity in the same way as predicted by the models, whatever the suction was. Similarly, the laboratory experiments suggest that stones reduce the unsaturated hydraulic conductivity while laboratory experiments in saturated conditions indicated that stones content might increase the K_{se}. These elements support the hypothesis of the macropore creation: according to the well-known law of Jurin (1717), pores through which water will flow depend both on the pore size distribution and the effective saturation. Consequently, flow in the macropore system will only be "activated" in the near-saturation zone while small pores will only be drained at high suction. Therefore, we could hypothesize that stones are always expected to decrease the hydraulic conductivity at low effective saturation states. However, under saturated conditions, relationship between R_v and K_{se} seems to be less trivial and requires further investigations considering soil texture and stone characteristics.

4. Conclusion

Determining the effect of rock fragments on soil hydraulic properties is a major issue in soil physics and in the study of fluxes in soil-plant-atmosphere systems in general. Several models aim at linking the hydraulic properties of fine earth to those of stony soil. Many of them assume that the only effect of stones is to reduce the volume available for water flow. We tested the validity of such models with various complementary experiments.

Our results suggest that considering that stones only reduce the volume available for water flow may be ill-founded. First, we observed that, contradictory to the predictive models, the saturated hydraulic conductivity of the clayey soil of this study increases with stone content. Besides, we pointed out several other potential drivers influencing K_{se}, which are not considered by these K_{se} predictive models. We observed that, for a given stoniness, the

resistance to flow is higher for smaller inclusions than for bigger ones. We explain this tendency by an overlapping of the influence zones of each stone combined with a higher tortuosity of the flow path. We also pointed out the shape of stones as a factor affecting the hydraulic conductivity of the soil. We showed that the effect of the shape depends on the inclusion size and inversely that the effect of inclusion size depends on its shape. Finally, our results converge to the assumption that this contradictory variation of K_{se} could find its origin at the creation of voids at the stone-fine earth interface as pointed out by Ravina and Magier (1984). Even if the very mechanisms behind these observations remains unclear, they seem to strongly depend on R_v, shape and roughness of inclusions. However, as we conducted these experiments on a specific clay soil only, and given the fact that structural modifications are textural dependent, our results can't be extrapolated to other soil textures without similar experiments. Finally, as we worked with disturbed samples, our results do not include quantification of natural phenomenon such as swelling and shrinking that occurs naturally for clay soils.

These findings suggest that the aforementioned predictive models are not appropriate in all cases, particularly under saturated conditions. Models should take into account the counteracting factors, notably size and shape of stones. However, further investigations are required in order to explore the hydraulic properties of stony soils and to develop new models or adapt the existing ones. The direct observation of undisturbed stony samples porosity using X-ray computed tomography or magnetic resonance imaging could confirm - at first - and then help better understand the mechanism of supposed voids creation at the stone-fine earth interface. However, under unsaturated conditions, these considerations should be more nuanced, as both numerical simulations and laboratory experiments corroborate the general trends from the predictive models. Finally, similar analyses should be conducted in view of determining the effect of the fine earth texture on the drivers of hydraulic properties as pointed out throughout our research.

Acknowledgements

We thank Stephane Becquevort of the soil physics lab for his support in setting up the experiments. The laboratory measurements of this study will be available upon publication of the paper at doi:10.5281/zenodo.32661.

References

Bouwer, H., and Rice, R.C. (1984). Hydraulic Properties of Stony Vadose Zones. Ground Water *22*, 696–705.

Brakensiek, D.L., Rawls, W.J., and Stephenson, G.R. (1986). Determining the Saturated Hydraulic Conductivity of a Soil Containing Rock Fragments1. Soil Sci. Soc. Am. J. *50*, 834.

Buchter, B., Hinz, C., and Flühler, H. (1994). Sample size for determination of coarse fragment content in a stony soil. Geoderma *63*, 265–275.

Corring, and Churchill, S.W. (1961). Chem. Eng. Prog. *57*, 53–59.

Cousin, I., Nicoullaud, B., and Coutadeur, C. (2003). Influence of rock fragments on the water retention and water percolation in a calcareous soil. Catena *53*, 97–114.

García-Ruiz, J.M. (2010). The effects of land uses on soil erosion in Spain: A review. CATENA *81*, 1–11.

Gusev, Y., and Novák, V. (2007). Soil water - main water resources for terrestrial ecosystems of the biosphere. J. Hydrol. Hydromech. Slovak Repub.

Hlaváčiková, H., and Novák, V. (2014). A relatively simple scaling method for describing the unsaturated hydraulic functions of stony soils. J. Plant Nutr. Soil Sci. *177*, 560–565.

Jurin, J. (1717). An Account of Some Experiments Shown before the Royal Society; With an Enquiry into the Cause of the Ascent and Suspension of Water in Capillary Tubes. Philos. Trans. *30*, 739–747.

Ma, D.H. and Shao, M.A.: Simulating infiltration into stony soils with a dual-porosity model, Eur. J. Soil Sci., 59, 950–959, 2008.

Ma, D.H., Zhang, J.H., Shao, M.A. and Wang, Q.J.: Validation of an analytical method for determining soil hydraulic properties of stony soils using experimental data, Geoderma,159, 262–269, 2010.

Miller, F.T., and Guthrie, R.L. (1984). Classification and distribution of soils containing rock fragments in the United States. Eros. Product. Soils Contain. Rock Fragm. SSSA Spec Publ *13*, 1–6.

Mohrath, D., Bruckler, L., Bertuzzi, P., Gaudu, J.C., and Bourlet, M. (1997). Error Analysis of an Evaporation Method for Determining Hydrodynamic Properties in Unsaturated Soil. Soil Sci. Soc. Am. J. *61*, 725.

Novák, V., and Kňava, K. (2011). The influence of stoniness and canopy properties on soil water content distribution: simulation of water movement in forest stony soil. Eur. J. For. Res. 1–9.

Novák, V., and Šurda, P. (2010). The water retention of a granite rock fragments in High Tatras stony soils. J. Hydrol. Hydromech. *58*, 181–187.

Novák, V., Kňava, K., and Šimůnek, J. (2011). Determining the influence of stones on hydraulic conductivity of saturated soils using numerical method. Geoderma *161*, 177–181.

Peck, A.J., and Watson, J.D. (1979). Hydraulic conductivity and flow in non-uniform soil.

Peters, A., and Durner, W. (2006). Improved estimation of soil water retention characteristics from hydrostatic column experiments. Water Resour. Res. *42*, W11401.

Peters, A., and Durner, W. (2008). Simplified evaporation method for determining soil hydraulic properties. J. Hydrol. *356*, 147–162.

Pichault, M. (2015). *Characterization of stony soil's hydraulic properties and elementary volume using field, laboratory and numerical experiments*. MsC thesis, ULg Gembloux Agro Bio Tech, 73 p

Poesen, J., and Lavee, H. (1994). Rock fragments in top soils: significance and processes. CATENA *23*, 1–28.

Ravina, I., and Magier, J. (1984). Hydraulic Conductivity and Water Retention of Clay Soils Containing Coarse Fragments. Soil Sci. Soc. Am. J. *48*, 736.

Russo, D. (1983). Leaching Characteristics of a Stony Desert Soil1. Soil Sci. Soc. Am. J. *47*, 431.

Sauer, and Logsdon (2002). Hydraulic and physical properties of stony soils in a small watershed. Soil Sci. Soc. Am. J. *66*.

Schindler, U. (1980). Ein Schnellverfahren zur Messung der Wasserleitfähigkeit im teilgesättigten Boden an Stechzylinderproben. Arch Acker- U Pflanzenbau U Bodenkd *24*, 1–7.

Schindler, U., and Müller, L. (2006). Simplifying the evaporation method for quantifying soil hydraulic properties. J. Plant Nutr. Soil Sci. *169*, 623–629.

Schindler, U., Durner, W., von Unold, G., and Müller, L. (2010). Evaporation Method for Measuring Unsaturated Hydraulic Properties of Soils: Extending the Measurement Range. Soil Sci. Soc. Am. J. *74*, 1071.

van Genuchten, M.T. (1980). A Closed-form Equation for Predicting the Hydraulic Conductivity of Unsaturated Soils. Soil Sci. Soc. Am. J. *44*, 892.Wendroth, E. (1993). Reevaluation of the evaporation method for determining hydraulic functions in unsaturated soils. Soil Sci. Soc. Am. J. *57*, 1436–1443.

Wind, G.P. (1968). Capillary conductivity data estimated by a simple method.

Zimmerman, R.W., and Bodvarsson, G.S. (1995). The effect of rock fragments on the hydraulic properties of soils (Lawrence Berkeley Lab., CA (United States). Funding organisation: USDOE, Washington, DC (United States)).

Zhou, B.B., Shao, M.A. and Shao, H.B.: Effects of rock fragments on water movement and solute transport in a Loess Plateau soil, Comptes Rendus Geosci., 341, 462–472, 2009.

Table 1 – Parameters of the van Genuchten equations used in the numerical experiments

θ_r [-]	θ_s [-]	α [cm^{-1}]	n [-]	l [-]	K_{se} [cm/day]
0.185	0.442	0.0064	2.11	-0.135	2.686

1

Table 2 – Schematic summary of the treatments

	Effect of R_v on unsaturated hydraulic conductivity		Effect of R_v on saturated hydraulic conductivity			Effect of size and shape on saturated hydraulic conductivity				
Method	Evaporation experiment + Permeameter		Permeameter			Permeameter				
R_v [%]	0 - 10 - 20 - 30	0 - 20	0 - 20 - 40 - 60			0 - 10 - 20 - 30				
Approach	Numerical	Laboratory	Numerical	Laboratory		Numerical				
Inclusion type	● (2D) n = 12	Rock fragments	● (2D) n = 12	Glass spheres	Rock fragments	● (2D) n = 1, 12, 27	▲ (2D) n = 1, 12, 27	▼ (2D) n = 1, 12, 27	▌ (2D) n = 1, 12, 27	▬ (2D) n = 1, 12, 27

1

Table 3 – Results from the investigation of the inclusion size and shape on the saturated hydraulic conductivity by means of numerical simulations (n is the number of inclusions simulated in the profile for the corresponding R_v)

		Relative saturated hydraulic conductivity		
R_v	Shape	n = 1	n = 12	n = 27
	▌	0.88	0.88	0.88
	●	0.84	0.83	0.82
	▲	0.80	0.79	0.78
	▼	0.80	0.79	0.78
10%	▬	0.84	0.83	0.82
	▌	0.76	0.71	0.68
	●	0.73	0.69	0.65
	▲	0.67	0.63	0.54
	▼	0.67	0.63	0.54
20%	▬	0.66	0.61	0.54
	▌	0.70	0.60	0.55
	●	0.64	0.58	0.48
	▲	0.59	0.50	0.46
	▼	0.59	0.50	0.47
30%	▬	0.56	0.48	0.31

1
2

Fig. 1 – Preparation of disturbed samples containing glass balls (left) and gravels (right).

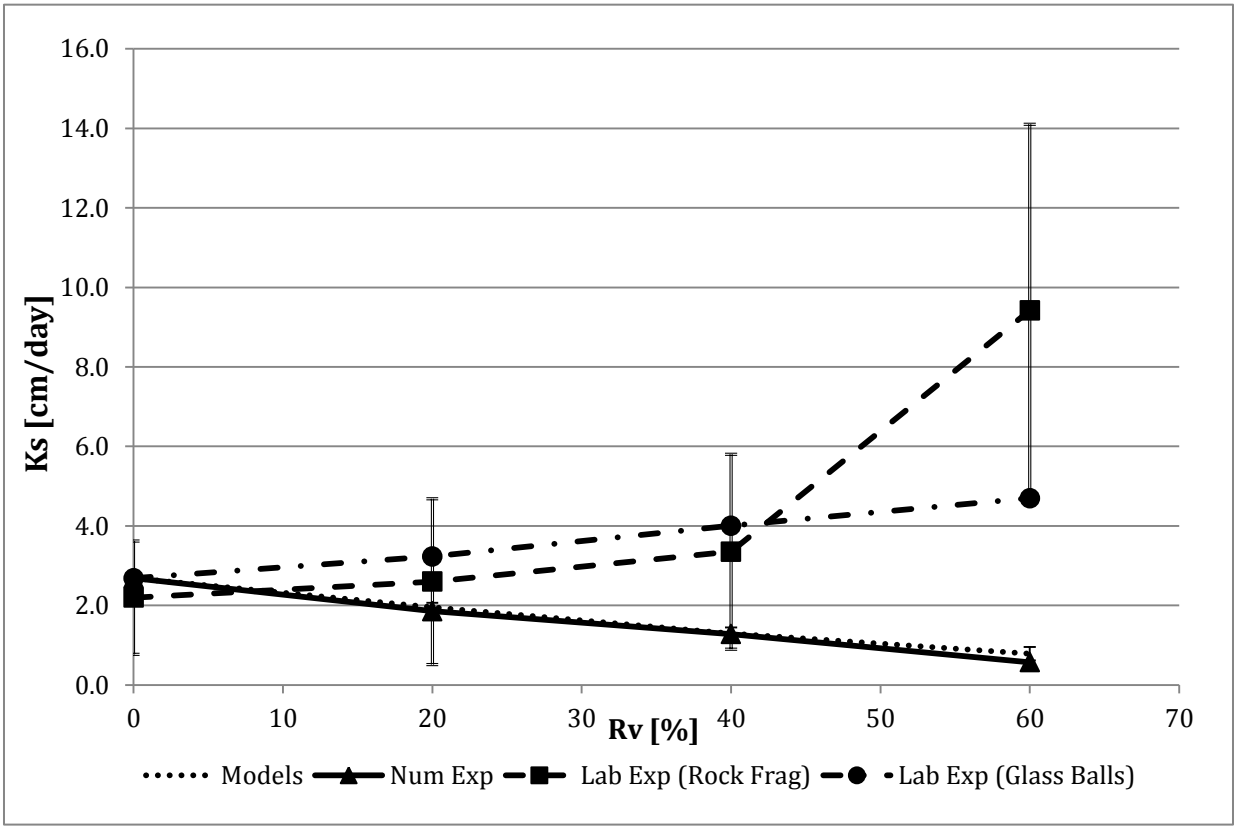

Fig. 2 – $\mathbf{K_{se}}$ depending on $\mathbf{R_v}$ obtained from laboratory experiments, numerical simulations with 12 circular inclusions and the predictive models (the bars show the 95% intervals around the median predicted by these models)

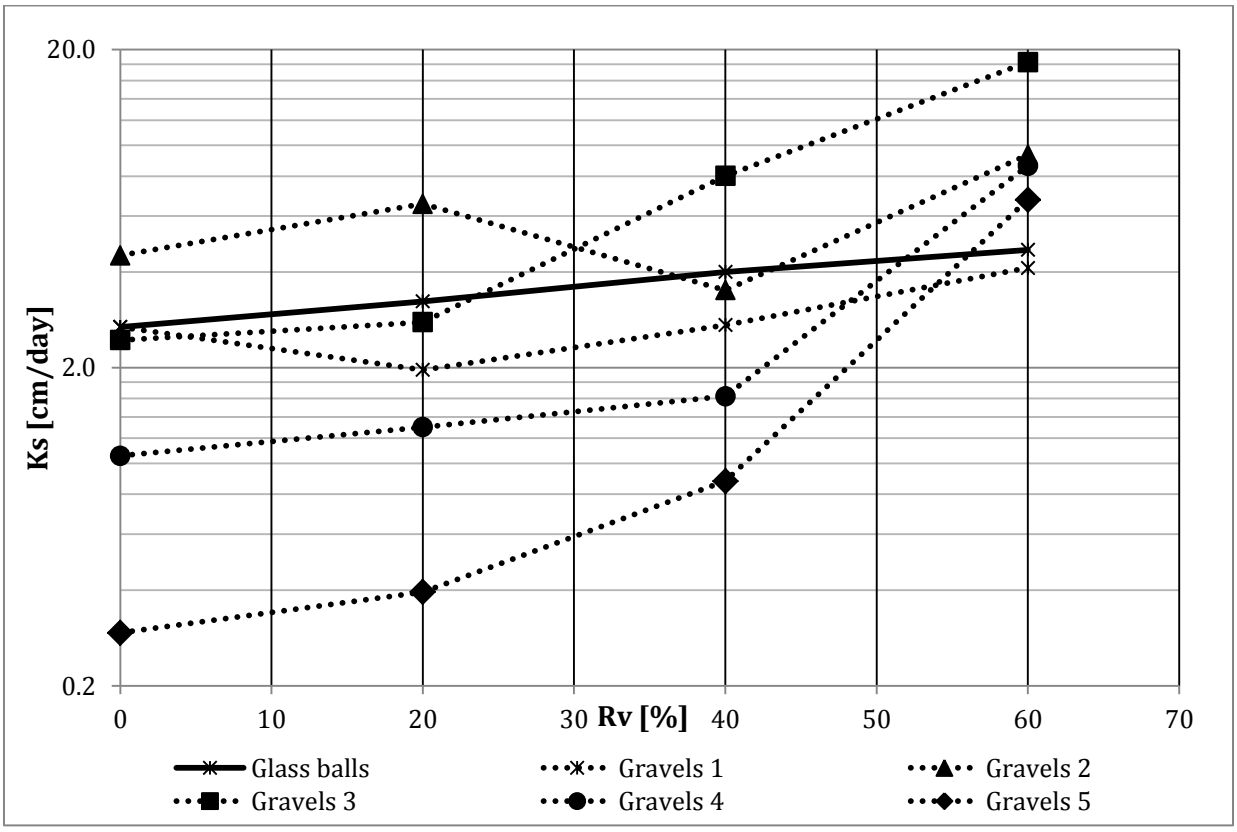

Fig. 3 – $\mathbf{K_{se}}$ depending on $\mathbf{R_v}$ obtained from laboratory experiments with gravels (5 replications) and glass balls (1 replication).

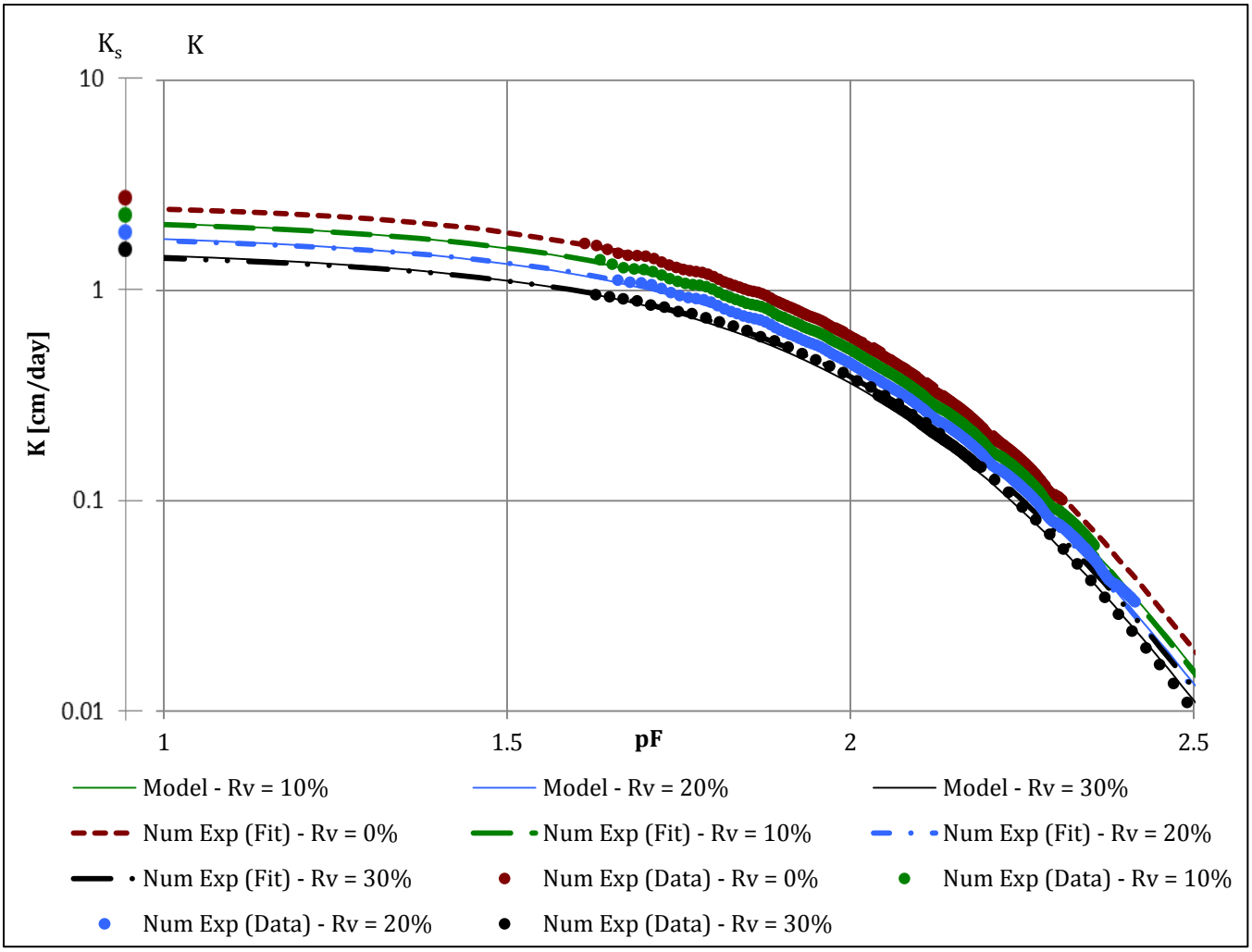

Fig. 4 – Hydraulic conductivity curves obtained from numerical experiments (data and fit for $\mathbf{R_v}$ = 0, 10, 20, 30%) and results predicted by the models for the coresponding $\mathbf{R_v}$

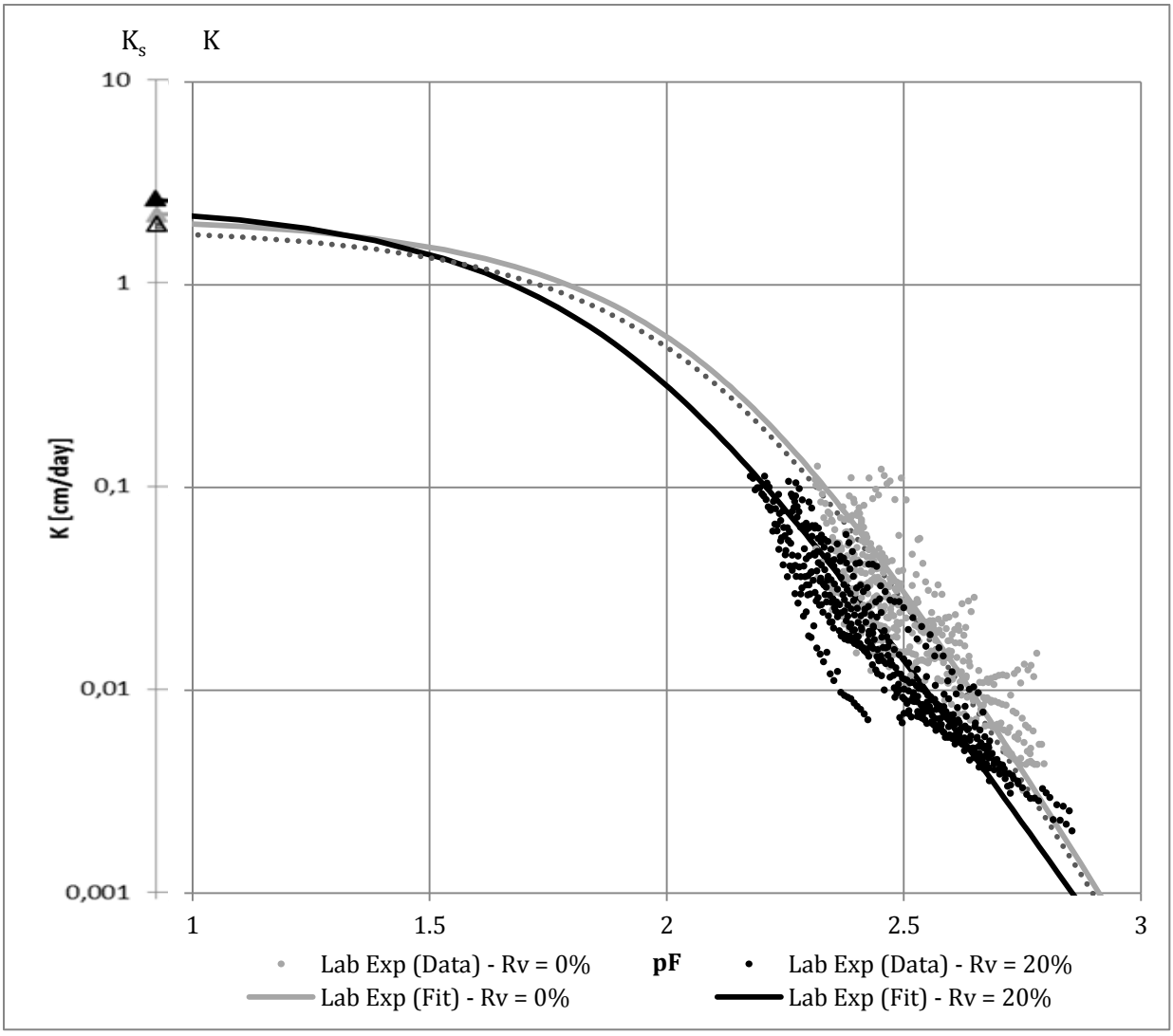

Fig. 5 – Hydraulic conductivity curves obtained from laboratory experiments (data and fit for R_v = 0 and 20%) and results predicted by the models for a R_v of 20%